Manuscript prepared for Nonlin. Processes Geophys.
with version 5.0 of the LaTeX class copernicus.cls.
Date: 17 May 2014

Estimation of the total magnetization direction of approximately spherical bodies

D. P. Sales[1], **V. C. Oliveira Jr.**[1], **V. C. F. Barbosa**[1], **and L. Uieda**[1, 2]

[1]Observatório Nacional, Brazil
[2]Universidade do Estado do Rio de Janeiro, Brazil

Correspondence to: V. C. Oliveira Jr.
(vandscoelho@gmail.com)

Abstract. TEXT

1 Introduction

TEXT

2 Methodology

2.1 Parameterization and Forward Problem

Let $\boldsymbol{\Delta T}^o$ be the observed data vector, whose ith element ΔT_i^o, $i = 1, ..., N$, is the total field anomaly measured at the position (x_i, y_i, z_i) (black dots in Fig. 1). In this Cartesian coordinate system, x points to geographic North, y points to East and z points downward. In general, the total field anomaly is produced by a magnetized susceptibility distribution which is anomalous with respect to the mean susceptibility of the crust. Mathematically, ΔT_i^o can be written as

$$\Delta T_i^o = \|\boldsymbol{T}_i\| + \|\boldsymbol{F}_i\| \,, \tag{1}$$

where $\|\|$ indicates the Euclidean norm, $\boldsymbol{F}_i$ is the Geomagnetic field vector and $\boldsymbol{T}_i$ is the Total Field, both at (x_i, y_i, z_i). The Total Field vector can be represented by the sum

$$\boldsymbol{T}_i = \boldsymbol{F}_i + \boldsymbol{B}_i \,, \tag{2}$$

where $\boldsymbol{B}_i$ is the Total Magnetic Induction vector produced by all magnetic sources (magnetized anomalous susceptibility distribution) at the position (x_i, y_i, z_i) (Blakely, 1996; Langel and Hinze, 1998).

For local or regional scale magnetic studies, it is very common to consider that (i) the Geomagnetic Field $\boldsymbol{F}_i$ (Eq. 1) is a constant vector $\boldsymbol{F}_0$ throughout the study area and (ii) that $\|\boldsymbol{F}_0\| \gg \|\boldsymbol{B}_i\|$, $i = 1, ..., N$ (Telford et al., 1990; Blakely, 1996). The second assumption is equivalent to say that the Total Magnetic Induction $\boldsymbol{B}_i$ (Eq. 1) is a small perturbation of the Geomagnetic field throughout the study area. These two assumptions make possible to approximate the Euclidean norm of the Total Field vector $\boldsymbol{T}_i$ (Eq. 1) by a first-order Taylor's expansion as follows

$$\begin{aligned} \|\boldsymbol{T}_i\| &\approx \|\boldsymbol{F}_0 + \boldsymbol{B}_i\| \\ &\approx \|\boldsymbol{F}_0\| + \hat{\boldsymbol{F}}^\intercal \boldsymbol{B}_i \,, \end{aligned} \tag{3}$$

where $^\intercal$ indicates transposition and

$$\hat{\boldsymbol{F}} = \frac{\boldsymbol{F}_0}{\|\boldsymbol{F}_0\|} \tag{4}$$

is a unit vector (with the same direction of the Geomagnetic field) representing the gradient of the function $\|\boldsymbol{T}_i\|$ with respect to the components of the vector $\boldsymbol{T}_i$ (Blakely, 1996). By introducing this first-order Taylor's expansion into the total field magnetic anomaly (Eq. 1), we obtain an approximated total field anomaly given by

$$\Delta T_i \approx \hat{\boldsymbol{F}}^\intercal \boldsymbol{B}_i \,, \qquad i = 1, ..., N \,. \tag{5}$$

Lets consider that the magnetic sources can be represented by a set of L uniformly magnetized spheres. In this case, the Total Magnetic Induction $\boldsymbol{B}_i$ is given by

$$\boldsymbol{B}_i = \sum_{j=1}^{L} \boldsymbol{b}_i^j \,, \tag{6}$$

being $\boldsymbol{b}_i^j$ the magnetic induction produced, at the position (x_i, y_i, z_i), by the jth sphere, $j = 1, ..., L$, with radius R_j (dashed straight lines in Fig. 1), centre at (xc_j, yc_j, zc_j) (grey

dots in Fig. 1) and magnetization vector $\boldsymbol{m}^j$ given by

$$\boldsymbol{m}^j = \begin{bmatrix} mx_j \\ my_j \\ mz_j \end{bmatrix}_{3\times 1} . \tag{7}$$

The magnetic induction $\boldsymbol{b}_i^j$ can be written as

$$\boldsymbol{b}_i^j = C_m \, \mathbf{M}_i^j \, \frac{4}{3}\pi R_j^3 \, \boldsymbol{m}^j \, , \tag{8}$$

where C_m is a constant given by $\mu_0/4\pi = 10^{-7}\ \frac{H}{m}$, μ_0 is the vacuum permeability and $\mathbf{M}_i^j$ is the matrix

$$\mathbf{M}_i^j = \begin{bmatrix} \frac{\partial^2}{\partial x \partial x}\frac{1}{r_j} & \frac{\partial^2}{\partial x \partial y}\frac{1}{r_j} & \frac{\partial^2}{\partial x \partial z}\frac{1}{r_j} \\ \frac{\partial^2}{\partial x \partial y}\frac{1}{r_j} & \frac{\partial^2}{\partial y \partial y}\frac{1}{r_j} & \frac{\partial^2}{\partial y \partial z}\frac{1}{r_j} \\ \frac{\partial^2}{\partial x \partial z}\frac{1}{r_j} & \frac{\partial^2}{\partial y \partial z}\frac{1}{r_j} & \frac{\partial^2}{\partial z \partial z}\frac{1}{r_j} \end{bmatrix}_{3\times 3} , \tag{9}$$

whose elements are the second derivatives, evaluated at the position (x_i, y_i, z_i), of the function

$$\frac{1}{r_j} \equiv \frac{1}{\sqrt{(x - xc_j)^2 + (y - yc_j)^2 + (z - zc_j)^2}} \tag{10}$$

with respect to the variables x, y and z. Blakely (1996) gives an expression equivalent to Eq. (8). By substituting the magnetic induction $\boldsymbol{b}_i^j$ (Eq. 8) into the Total Magnetic Induction vector (Eq. 6) and using the approximated total field anomaly (Eq. 5) we may then obtain the total field anomaly predicted by the set of L spheres at the position (x_i, y_i, z_i), $i = 1, ..., N$, as follows

$$\begin{aligned} d_i(\boldsymbol{h}) &= \hat{\boldsymbol{F}}^\intercal \textstyle\sum_{j=1}^{L} \mathbf{M}_i^j \, \boldsymbol{h}^j \\ &= \boldsymbol{a}_i^\intercal \boldsymbol{h} \, , \end{aligned} \tag{11}$$

where

$$\boldsymbol{h}^j = C_m \, \frac{4}{3}\pi R_j^3 \, \boldsymbol{m}^j \, , \qquad j = 1, ..., L \, , \tag{12}$$

$$\boldsymbol{h} = \begin{bmatrix} \boldsymbol{h}^1 \\ \vdots \\ \boldsymbol{h}^L \end{bmatrix}_{3L\times 1} , \tag{13}$$

and

$$\boldsymbol{a}_i = \begin{bmatrix} \mathbf{M}_i^1 \, \hat{\boldsymbol{F}} \\ \vdots \\ \mathbf{M}_i^L \, \hat{\boldsymbol{F}} \end{bmatrix}_{3L\times 1} . \tag{14}$$

Finally, let $\boldsymbol{d}(\boldsymbol{h})$ be the predicted data vector, whose ith element $d_i(\boldsymbol{h})$, $i = 1, ..., N$, (Eq. 11) is the total field anomaly predicted by the set of L spheres at the position (x_i, y_i, z_i) (black dots in Fig. 1). By using Eq. (11), the predicted data vector $\boldsymbol{d}(\boldsymbol{h})$ can be written as

$$\boldsymbol{d}(\boldsymbol{h}) = \mathbf{A} \, \boldsymbol{h} \, , \tag{15}$$

where $\mathbf{A}$ is an $N \times 3L$ matrix given by

$$\mathbf{A} = \begin{bmatrix} \boldsymbol{a}_1^\intercal \\ \vdots \\ \boldsymbol{a}_N^\intercal \end{bmatrix}_{N\times 3L} , \tag{16}$$

being $\boldsymbol{a}_i$, $i = 1, ..., N$, defined in Eq. (14) and $\boldsymbol{h}$ shown in Eq. 13.

2.2 Inverse Problem

Equation (15) shows that the predicted data vector depends on the parameter vector $\boldsymbol{h}$ (Eq. 13), which is formed by all vectors $\boldsymbol{h}^j$, $j = 1, ..., L$, (Eq. 12). Note that $\boldsymbol{h}^j$ (Eq. 12) has the same direction as the magnetization vector $\boldsymbol{m}^j$ of the jth sphere, $j = 1, ..., L$ (Eq. 7). Consequently, the predicted data vector $\boldsymbol{d}(\boldsymbol{h})$ depends on the magnetization direction of all L spheres. Hence, by presuming that the magnetic sources producing the observed data $\boldsymbol{\Delta T}^o$ can be represented by a set of L uniformly magnetized spheres, we can calculate the magnetization direction of all L spheres by estimating the parameter vector $\hat{\boldsymbol{h}}$ that minimizes the goal function

$$\Psi(\boldsymbol{h}) = \frac{1}{N}[\boldsymbol{\Delta T}^o - \boldsymbol{d}(\boldsymbol{h})]^\intercal [\boldsymbol{\Delta T}^o - \boldsymbol{d}(\boldsymbol{h})] \, . \tag{17}$$

The parameter vector $\hat{\boldsymbol{h}}$ minimizing the goal function (Eq. 17) satisfies the following condition

$$\boldsymbol{g}(\hat{\boldsymbol{h}}) = \mathbf{0} \tag{18}$$

where $\boldsymbol{g}(\hat{\boldsymbol{h}})$ is the gradient vector, evaluated at $\hat{\boldsymbol{h}}$, of the goal function $\Psi(\boldsymbol{h})$ (Eq. 17) and $\mathbf{0}$ is a vector with null elements. Equation (18) leads to the Least-Squares estimate $\hat{\boldsymbol{h}}$ of the parameter vector $\boldsymbol{h}$ (Eq. 13)

$$\hat{\boldsymbol{h}} = (\mathbf{A}^\intercal \mathbf{A})^{-1} \mathbf{A}^\intercal \, \boldsymbol{\Delta T}^o \, . \tag{19}$$

In practice, instead of solving the Eq. (19), the matrix $(\mathbf{A}^\intercal \mathbf{A})$ is not inverted and the estimate $\hat{\boldsymbol{h}}$ is obtained by solving the resulting linear system. By presuming the existence of $(\mathbf{A}^\intercal \mathbf{A})^{-1}$, Eq. (17) gives an estimate $\hat{\boldsymbol{h}}$ producing the predicted data $\boldsymbol{d}(\hat{\boldsymbol{h}})$ (Eq. 15) as near as possible from the observed data $\boldsymbol{\Delta T}^o$, in the Least-Squares sense (Bard, 1973; Twomey, 1977; Menke, 1989; Aster et al., 2005).

The estimated parameter vector $\hat{\boldsymbol{h}}$ (Eq. 19) obtained by using Least Squares is very sensitive to outliers in the observed data. In some cases, if the outliers are not properly removed from the observed data, the estimated parameters can be seriously misleading. When working with field data, these outliers can be caused by, for example, interfering magnetic sources or cultural noise. In order to deal with this problem in an automatic manner, instead of using the Least Squares estimate $\hat{\boldsymbol{h}}$ (Eq. 19), we can use a robust scheme for estimating the parameter vector $\tilde{\boldsymbol{h}}$ minimizing the goal function

$$\Gamma(\boldsymbol{h}) = \frac{1}{N} \sum_{i=1}^{N} |\Delta T_i^o - d_i(\boldsymbol{h})| \, . \tag{20}$$

Similarly to the Least Squares estimate $\hat{\boldsymbol{h}}$ (Eq. 19), the vector $\tilde{\boldsymbol{h}}$ minimizing the goal function $\Gamma(\boldsymbol{h})$ (Eq. 20) satisfies the condition

$$\boldsymbol{q}(\tilde{\boldsymbol{h}}) = \mathbf{0} \tag{21}$$

where $\boldsymbol{q}(\tilde{\boldsymbol{h}})$ is the gradient vector, evaluated at $\tilde{\boldsymbol{h}}$, of the goal function $\Gamma(\boldsymbol{h})$ (Eq. 20) and $\mathbf{0}$ is a vector with null elements. Different from Eq. (18), Eq. (20) leads to a system of non-linear equations for obtaining the vector $\tilde{\boldsymbol{h}}$ (Robust estimate) minimizing the goal function $\Gamma(\boldsymbol{h})$ (Eq. 20). While the Least Squares estimate $\hat{\boldsymbol{h}}$ is directly obtained by solving the Eq. (19), the Robust estimate $\tilde{\boldsymbol{h}}$ is obtained iteratively by solving, at each iteration, the linear system

$$\left(\mathbf{A}^\intercal \mathbf{R}^k \mathbf{A}\right) \boldsymbol{h}^{k+1} = \mathbf{A}^\intercal \mathbf{R}^k \boldsymbol{\Delta T}^o \,, \tag{22}$$

where $\mathbf{R}^k$ is a diagonal $N \times N$ matrix whose ith element r_i^k, $i = 1, ..., N$, is given by

$$r_i^k = \frac{1}{|\Delta T_i^o - d_i(\boldsymbol{h}^k) + \epsilon|} \,, \tag{23}$$

being ϵ a small positive number used for dealing with singularities when $\Delta T_i^o = d_i(\boldsymbol{h}^k)$. This iterative process begins with $\boldsymbol{h}^0 = \hat{\boldsymbol{h}}$, being $\hat{\boldsymbol{h}}$ the Least Squares estimate (Eq. 19). By using the initial approximation $\boldsymbol{h}^0$, we calculate the matrix $\mathbf{R}^0$ and solve the linear system given by Eq. (22) for obtaining the estimate $\boldsymbol{h}^1$. This procedure is repeated for obtaining the estimate $\boldsymbol{h}^2$ and so on. After some iterations, this iterative procedure converges to an approximation of the Robust estimate $\tilde{\boldsymbol{h}}$ minimizing the goal function $\Gamma(\boldsymbol{h})$ (Eq. 20). This algorithm is named Iteratively Reweighted Least Squares (Scales et al., 1988; Aster et al., 2005).

Both $\hat{\boldsymbol{h}}$ (Least Squares estimate) and $\tilde{\boldsymbol{h}}$ (Robust estimate) are estimates of the parameter vector $\boldsymbol{h}$ (Eq. 13). The parameter vector is represented in Cartesian coordinates as a function of the elements $h\alpha_j$, $\alpha = x, y, z$, $j = 1, ..., L$, of the vectors $\boldsymbol{h}^j$ (Eq. 12), which in turn are functions of the elements $m\alpha_j$, $\alpha = x, y, z$, $j = 1, ..., L$, of the magnetization vector $\boldsymbol{m}^j$ (Eq. 7). However, the magnetization vector is commonly represented in terms of its intensity, declination and inclination. Therefore, for convenience, we will represent the vector $\hat{\boldsymbol{h}}^j$ (Eq. 12) in spherical coordinates as follows

$$\boldsymbol{h}^j = Q_j \begin{bmatrix} \cos I_j \, \cos D_j \\ \cos I_j \, \sin D_j \\ \sin I_j \end{bmatrix}_{3\times 1} \,, \tag{24}$$

where the intensity Q_j, declination D_j and inclination I_j are given as functions of the elements $h\alpha_j$, $\alpha = x, y, z$ (Fig. 2), by

$$Q_j = \sqrt{hx_j^2 + hy_j^2 + hz_j^2} \quad , \tag{25}$$

$$D_j = \arctan\left(\frac{hy_j}{hx_j}\right) \quad , \tag{26}$$

$$I_j = \arctan\left(\frac{hz_j}{\sqrt{hx_j^2 + hy_j^2}}\right) \quad . \tag{27}$$

So, after obtaining an estimated parameter vector (Least Squares or Robust estimate), we use the Eq(s). (26) and (27) for calculating, respectively, the declinations D_j and inclinations I_j, $j = 1, ..., L$, of the total magnetization vector of all spheres. For convenience, the symbol $\hat{}$ is used to denote declinations $\hat{D}_j$ and inclinations $\hat{I}_j$, $j = 1, ..., L$, calculated by using the elements of the Least Squares estimate $\hat{\boldsymbol{h}}$ (Eq. 17). Similarly, the symbol $\tilde{}$ denotes that the declinations $\tilde{D}_j$ and inclinations $\tilde{I}_j$, $j = 1, ..., L$, are calculated by using the elements of the Robust estimate $\tilde{\boldsymbol{h}}$ produced by the iterative process (Eqs. 22 and 23).

2.3 Uncertainty of the estimated parameters

Total field anomaly measurements obtained in a geophysical survey are always affected by some noise. This noise is due to the wide range of experimental errors and inaccuracies that happens in a geophysical survey. Additionally, the noise makes impossible obtaining the same observed total field anomaly, even if all experimental conditions of the survey were exactly reproduced. The noise in the observed data $\boldsymbol{\Delta T}^o$ affects the estimated parameter vector, independently of the used method. Therefore, it is necessary to quantify this effect by propagating the uncertainty from the observed data to the estimated parameter vector. Here, this error propagation is done by using the covariance matrix (Bard, 1973; Aster et al., 2005). The covariance matrix $\hat{\mathbf{C}}$ of the Least Squares estimate $\hat{\boldsymbol{h}}$ (Eq. 19) is given as a function of the covariance matrix $\mathbf{D}$ of the observed data. By presuming that the errors of all observed data ΔT_i^o, $i = 1, ..., N$, are independent and of equal variance σ^2, we obtain $\mathbf{D} = \sigma^2 \mathbf{I}$, where $\mathbf{I}$ is the $N \times N$ identity matrix. From this assumption, we obtain

$$\hat{\mathbf{C}} = \hat{\mathbf{H}} \, \mathbf{D} \, \hat{\mathbf{H}}^\intercal \,, \tag{28}$$

where

$$\hat{\mathbf{H}} = \left(\mathbf{A}^\intercal \mathbf{A}\right)^{-1} \mathbf{A}^\intercal \,. \tag{29}$$

Similarly, the covariance matrix $\tilde{\mathbf{C}}$ of the Robust estimate $\tilde{\boldsymbol{h}}$ (Eqs. 22 and 23) can be given by

$$\tilde{\mathbf{C}} = \tilde{\mathbf{H}} \, \mathbf{D} \, \tilde{\mathbf{H}}^\intercal \,, \tag{30}$$

where

$$\tilde{\mathbf{H}} = \left(\mathbf{A}^\intercal \mathbf{R}^k \mathbf{A}\right)^{-1} \mathbf{A}^\intercal \mathbf{R}^k \,, \tag{31}$$

being the matrix $\mathbf{R}^k$ (Eqs. 22 and 23) the last one calculated in the iterative process for estimating $\tilde{\boldsymbol{h}}$ (Bard, 1973; Aster et al., 2005).

The diagonal of the matrices $\hat{\mathbf{C}}$ (Eq. 28) and $\tilde{\mathbf{C}}$ (Eq. 30) contain the variances of the elements of the Least Squares

estimate $\hat{\boldsymbol{h}}$ (Eq. 19) and Robust estimate $\tilde{\boldsymbol{h}}$ (Eqs. 22 and 23), respectively. Let $\boldsymbol{v}$ be a $3L$-dimensional vector whose element v_j, $j = 1, ..., 3L$ represents the jth element of the diagonal of the covariance matrix $\hat{\mathbf{C}}$ (Eq. 28) or $\tilde{\mathbf{C}}$ (Eq. 30). This vector can be represented by

$$\boldsymbol{v} = \begin{bmatrix} \boldsymbol{v}^1 \\ \vdots \\ \boldsymbol{v}^L \end{bmatrix}_{3L\times 1}, \tag{32}$$

where

$$\boldsymbol{v}^j = \begin{bmatrix} (\sigma x_j)^2 \\ (\sigma y_j)^2 \\ (\sigma z_j)^2 \end{bmatrix}_{3\times 1}, \tag{33}$$

being $\sigma\alpha_j$, $\alpha = x, y, z$, $j = 1, ..., L$, the uncertainty of the component $h\alpha_j$, $\alpha = x, y, z$, $j = 1, ..., L$, of the vector $\boldsymbol{h}^j$ (Eq. 12) forming the estimated parameter vector. For convenience, the symbol $\hat{}$ is used to denote uncertainties $\hat{\sigma\alpha}_j$, $\alpha = x, y, z$, $j = 1, ..., L$, calculated by using the elements of the Least Squares estimate $\hat{\boldsymbol{h}}$ (Eq. 17). Similarly, the symbol $\tilde{}$ denotes that the uncertainties $\tilde{\sigma\alpha}_j$, $\alpha = x, y, z$, $j = 1, ..., L$, are calculated by using the elements of the Robust estimate $\tilde{\boldsymbol{h}}$ produced by the iterative process (Eqs. 22 and 23).

In the previous section, for convenience, we describe the vectors $\boldsymbol{h}^j$, $j = 1, ..., L$ (Eq. 12), in terms of its intensity Q_j (Eq. 25), declination D_j (Eq. 26) and inclination I_j (Eq. 27), as shown in Fig. (2). This quantities are described as functions of the components $h\alpha_j$, $\alpha = x, y, z$, $j = 1, ..., L$, of the vector $\boldsymbol{h}^j$. Therefore, the uncertainty of the intensity Q_j, declination D_j and inclination I_j can be given as functions of the uncertainties $\sigma\alpha_j$, $\alpha = x, y, z$, $j = 1, ..., L$ shown in Eq. (33). To do it, we presume that the components $h\alpha_j$, $\alpha = x, y, z$, $j = 1, ..., L$, of the vector $\boldsymbol{h}^j$ (Eq. 12) are statistically independent and use the propagation of uncertainties (Fornasini, 2008). From this assumption, the uncertainties σ_{Qj}, σ_{Dj} and σ_{Ij} of the intensity Q_j (Eq. 25), declination D_j (Eq. 26) and inclination I_j (Eq. 27), respectively, are given by

$$\sigma_{Qj} = \sqrt{\left(\frac{\partial Q_j}{\partial hx_j}\,\sigma x_j\right)^2 + \left(\frac{\partial Q_j}{\partial hy_j}\,\sigma y_j\right)^2 + \left(\frac{\partial Q_j}{\partial hz_j}\,\sigma z_j\right)^2}, \tag{34}$$

$$\sigma_{Dj} = \sqrt{\left(\frac{\partial D_j}{\partial hx_j}\,\sigma x_j\right)^2 + \left(\frac{\partial D_j}{\partial hy_j}\,\sigma y_j\right)^2} \tag{35}$$

and

$$\sigma_{Ij} = \sqrt{\left(\frac{\partial I_j}{\partial hx_j}\,\sigma x_j\right)^2 + \left(\frac{\partial I_j}{\partial hy_j}\,\sigma y_j\right)^2 + \left(\frac{\partial I_j}{\partial hz_j}\,\sigma z_j\right)^2}. \tag{36}$$

The first-order derivatives shown in Eqs. (34), (35) and (36) are given by

$$\frac{\partial Q_j}{\partial h\alpha_j} = \frac{h\alpha_j}{Q_j}, \quad \alpha = x, y, z, \tag{37}$$

$$\frac{\partial D_j}{\partial hx_j} = \frac{-hy_j}{(hx_j)^2 + (hy_j)^2}, \tag{38}$$

$$\frac{\partial D_j}{\partial hy_j} = \frac{hx_j}{(hx_j)^2 + (hy_j)^2}, \tag{39}$$

$$\frac{\partial I_j}{\partial h\alpha_j} = \frac{-h\alpha_j hz_j}{Q_j^2\sqrt{(hx_j)^2 + (hy_j)^2}}, \quad \alpha = x, y, \tag{40}$$

and

$$\frac{\partial I_j}{\partial hz_j} = \frac{\sqrt{(hx_j)^2 + (hy_j)^2}}{Q_j^2}. \tag{41}$$

For convenience, the symbol $\hat{}$ is used to denote the uncertainties $\hat{\sigma}_{Qj}$, $\hat{\sigma}_{Dj}$ and $\hat{\sigma}_{Ij}$, $j = 1, ..., L$, calculated with the Eqs. (34), (35) and (36), respectively, by using the elements of the Least Squares estimate $\hat{\boldsymbol{h}}$ (Eq. 17). Similarly, the symbol $\tilde{}$ denotes that the uncertainties $\tilde{\sigma}_{Qj}$, $\tilde{\sigma}_{Dj}$ and $\tilde{\sigma}_{Ij}$, $j = 1, ..., L$, are calculated with the Eqs. (34), (35) and (36), respectively, by using the elements of the Robust estimate $\tilde{\boldsymbol{h}}$ produced by the iterative process (Eqs. 22 and 23).

3 Application to synthetic data

TEXT

3.1 Validation test

TEXT

3.2 Violation test

TEXT

3.3 Field-conditions test

TEXT

4 Application to field data

TEXT

5 Conclusions

TEXT

Acknowledgements. TEXT

References

Aster, R. C., Borchers, B., and Thurber, C. H.: Parameter Estimation and Inverse Problems (International Geophysics), Academic Press, 2005.

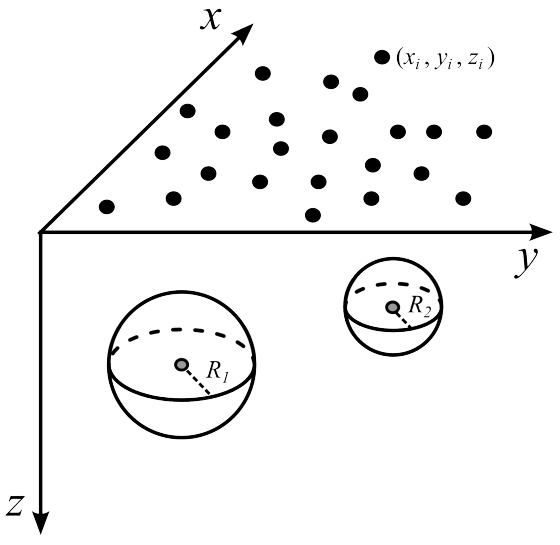

Fig. 1. Schematic representation of $L = 2$ spheres uniformly magnetized at the subsurface. These spheres have radii R_j (dashed straight lines), constant magnetization vectors $\boldsymbol{m}^j$ and centres (grey dots) at (xc_j, yc_j, zc_j), $j = 1, ..., L$. The total field anomaly produced by these spheres can be observed at the points (x_i, y_i, z_i), $i = 1, ..., N$ (black dots). In this Cartesian coordinate system, x points to the geographic North, y points to East and z points downward.

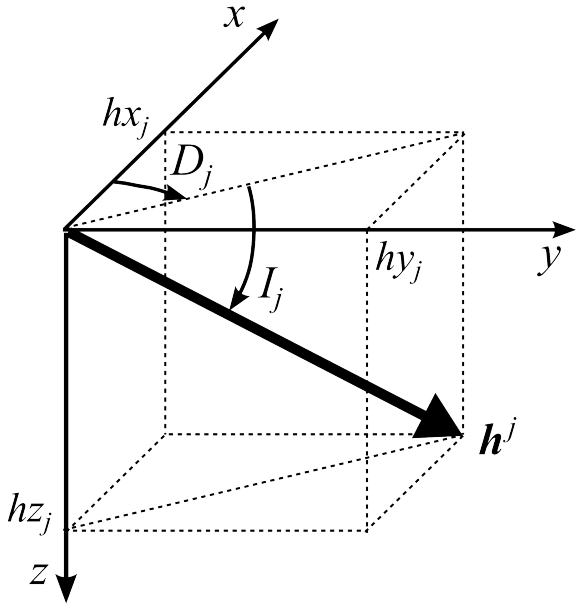

Fig. 2. Schematic representation of the vector $\boldsymbol{h}^j$ (Eq. 12) with elements hx_j, hy_j and hz_j described in Cartesian coordinates. This vector has a declination D_j (positive from x to y) and inclination I_j (positive downward), $j = 1, ..., L$.

Bard, Y.: Nonlinear Parameter Estimation, Academic Press, 1973.

Blakely, R. J.: Potential Theory in Gravity and Magnetic Applications, Cambridge University Press, 1996.

Fornasini, P.: The Uncertainty in Physical Measurements: An Introduction to Data Analysis in the Physics Laboratory, Springer, 2008.

Langel, R. A. and Hinze, W. J.: The Magnetic Field of the Earth's Lithosphere: The Satellite Perspective, Cambridge University Press, 1998.

Menke, W.: Geophysical Data Analysis: Discrete Inverse Theory (International Geophysics), Academic Press, 1989.

Scales, J. A., Gerztenkorn, A., and Treitel, S.: Fast Lp Solution of Large, Sparse, Linear Systems: Application to Seismic Travel Time Tomography, J. Comput. Phys., 75, 314–333, doi:10.1016/0021-9991(88)90115-5, 1988.

Telford, W. M., Geldart, L. P., and Sheriff, R. E.: Applied Geophysics, Cambridge University Press, 1990.

Twomey, S.: Introduction to the Mathematics of Inversion in Remote Sensing and Indirect Measurements, Dover Publications, Inc., 1977.